◆ Human Brain Mapping 38:1224–1232 (2017) ◆

The Role of the Pallidothalamic Fibre Tracts in Deep Brain Stimulation for Dystonia: A Diffusion MRI Tractography Study

Verena Eveline Rozanski,[1]* Nadia Moreira da Silva,[2] Seyed-Ahmad Ahmadi,[1] Jan Mehrkens,[3] Joao da Silva Cunha,[2] Jean-Christophe Houde,[4] Christian Vollmar,[1] Kai Bötzel,[1] and Maxime Descoteaux[4]

[1]Department of Neurology, Klinikum Grosshadern, University of Munich, Germany
[2]Department of Engineering, INESC TEC and Faculty of Engineering, University of Porto, Rua Dr. Roberto Frias, Porto 4200-465, Portugal
[3]Department of Neurosurgery, Klinikum Grosshadern, University of Munich, Germany
[4]Department of Computer Science, Sherbrooke Connectivity Imaging Lab (SCIL), Computer Science department, Université de Sherbrooke, Sherbrooke, Québec, Canada

Abstract: *Background:* Deep Brain Stimulation (DBS) of the Globus pallidus internus (GPi) is gold standard treatment in medically refractory dystonia. Recent evidence indicates that stimulation effects are also due to axonal modulation and affection of a fibre network. For the GPi, the pallidothalamic tracts are known to be the major motor efferent pathways. The aim of this study is to explore the anatomic vicinity of these tracts and DBS electrodes in dystonia applying diffusion tractography. *Methods:* Diffusion MRI was acquired in ten patients presenting for DBS for dystonia. We applied both a conventionally used probabilistic tractography algorithm (FSL) as well as a probabilistic streamline tracking approach, based on constrained spherical deconvolution and particle filtering with anatomic priors, to the datasets. DBS electrodes were coregistered to the diffusion datasets. *Results:* We were able to delineate the pallidothalamic tracts in all patients. Using the streamline approach, we were able to distinguish between the two sub-components of the tracts, the *ansa lenticularis* and the *fasciculus lenticularis*. Clinically efficient DBS electrodes displayed a close anatomic vicinity pathway of the pallidothalamic tracts, and their course was consistent with previous tracer labelling studies. Although we present only anatomic data, we interpret these findings as evidence of the possible involvement of fibre tracts to the clinical effect in DBS. Electrophysiological intraoperative recordings would be needed to complement our findings. In the future, a clear and individual delineation of the pallidothalamic tracts could optimize the stereotactic process of optimal electrode localization. *Hum Brain Mapp 38:1224–1232, 2017.* © 2016 Wiley Periodicals, Inc.

Key words: deep brain stimulation; movement disorders; diffusion MRI; neural networks

Additional Supporting Information may be found in the online version of this article.

*Correspondence to: Verena Eveline Rozanski, Department of Neurology, Klinikum Grosshadern, Marchioninistr. 15, 81377 Munich, Germany. E-mail: verenarozanski@med.uni-muenchen.de

Conflict of interest: none
Contract grant sponsor: Bavaria-Quebec-Office (http://www.baviere-quebec.org/).

Received for publication 25 February 2016; Revised 14 September 2016; Accepted 18 October 2016.

DOI: 10.1002/hbm.23450
Published online 16 November 2016 in Wiley Online Library (wileyonlinelibrary.com).

INTRODUCTION

Deep Brain Stimulation (DBS) is gold standard treatment in medically refractory movement disorders, for example, Parkinson's disease [Machado et al., 2006], essential tremor [Huss et al., 2015], and dystonia [Volkmann et al., 2014], but it is also increasingly applied for intractable epilepsy, pain, and psychiatric conditions [Kocabicak et al., 2015]. The modulation of axonal white matter bundles by stimulation current is being brought into focus and a number of fibre bundles have been identified and associated with stimulation targets and diseases [Klein et al., 2012; Vanegas-Arroyave et al., 2016]. Among these, the medial forebrain bundle and the anterior thalamic radiation have been identified as important pathways in DBS for depression [Coenen et al., 2012], whereas the dentato-rubro-thalamic tract was found to be a stereotactic target in essential tremor [Coenen et al., 2011]. Based on these findings, calls for tractography-guided stereotaxy [Hunsche et al., 2013; Lauro et al., 2016] have emerged.

In medically intractable dystonia, DBS electrodes are placed within the internal segment of the Globus pallidus, termed *GPi (GPi: Globus Pallidus internus)* [Volkmann et al., 2014]. Within the basal ganglia loop, the GPi constitutes an important relay station and main output structure of the basal ganglia [Parent and Hazrati, 1995] that is highly interconnected: it receives afferent fibres mainly from the nigropallidal and striatopallidal pathways and sends efferences to the thalamus via the pallidothalamic pathways [Beukema et al., 2015]. The pallidothalamic tract constitutes the major efferent fibre bundle of the GPi and is composed of the ventrally located ansa lenticularis and the more dorsal fasciculus lenticularis that later merge to form the fasciculus thalamicus [Gallay et al., 2008].

In a previous diffusion MRI study, we were able to show differences in remote connectivity profiles for clinically efficient and less efficient DBS electrodes [Rozanski et al., 2014]. Ventral and dorsal GPi segments displayed differences in cortical connectivity profiles, with the ventral GPi being more connected to the primary somatosensory cortex and posterior motor regions, and the dorsal GPi being connected more to anterior motor and premotor regions [Rozanski et al., 2014]. In accordance, stimulation of ventral and dorsal GPi produced opposite motor effects in Parkinsonian patients and this was attributed to the subdivision of the pallidothalamic tracts into its ventral and dorsal components [Krack et al., 1998]. These fibre bundles have not been analysed specifically in the previous paper.

The aim of this study is, therefore, to explore the role of the pallidothalamic tract as the major GPi efferent in DBS. We intend to delineate the course of the pallidothalamic tracts in ten dystonia patients presenting for DBS and, second, to analyse the topographic relationship between the clinically most efficient DBS electrode contact and the pallidothalamic tracts. To test the reliability of our results, we applied two tractography methods, one being the bedpostx FSL probabilistic tractography [Behrens et al., 2007], the other being a recent streamline probabilistic tractography based on constrained spherical deconvolution and anatomical priors [Girard et al., 2014].

Abbreviations

al	ansa lenticularis
ft	fasciculus thalamicus
fx	fornix;
lf	lenticular fasciculus
ot	optic tract
P.l.	Pars lateralis
P.m.	Pars medialis
Put	Putamen
R	Reticular nucleus
STN	Subthalamic nucleus
VA	ventral anterior nucleus
VApc	Ventral anterior nucleus, parvocellular division
VLa/p	Ventral lateral nucleus, anterior/posterior part
VM	ventral medial nucleus
ZI	Zona incerta

METHODS

This study was approved of by the local ethics committee, complying with the 1995 Declaration of Helsinki. Informed consent was obtained from all patients.

Clinical Setting

Ten patients with medically intractable focal and segmental dystonia presenting for DBS were included in the study. Patient details are given in Table I. DBS was performed as previously described in detail [Mehrkens et al., 2009]. In brief, Medtronic 3387 electrodes were implanted bilaterally into GPi in dystonia patients and connected to Activa PC neurostimulators. Correct electrode placement was verified on postoperative CT scans. Intraoperative microelectrode recording was performed to facilitate correct lead placement.

Selection of optimal stimulation electrode contact was performed in accordance to DBS guidelines [Kupsch et al., 2006, 2011]. For each patient, all contacts were stimulated up to a voltage of 3,5 V and tested for side-effects separately. After ruling out side effects, the most ventral contact was activated in a monopolar setting (frequency: 130 Hz, impulse duration: 120 μs) with an initial stimulation amplitude of 1.5 V, which was gradually increased according to clinical efficiency. A more dorsal contact was chosen, when capsular side effects, phosphenes or other side effects occurred before a reduction of dystonic symptoms was achieved. If no clinical benefit was achieved by monopolar stimulation of each electrode, a bipolar setting was chosen, starting with the activation of the two adjacent lowest electrode contacts, then proceeding to the higher electrode contacts. Regular re-evaluation and re-adjustment of stimulation parameters was performed in the outpatient department to ensure selection of best clinical contact. Severity of dystonia symptoms was evaluated according to the

TABLE I. Presents the clinical details of the patients enrolled in this study

Patient number	Age	Sex	Disease duration	Clinical phenotype of dystonia	BFMDRS[a] preoperative	BFMDRS[a] postoperative	Settings right stimulator 8 9 10 11	Settings left stimulator 0 1 2 3
1	40	m	10	Meige	15	2	−000, 2,6 V, 120 µs, 130 Hz	−000, 2,6 V, 120 µV 130 Hz
2	58	m	8	Cervical	4	0,5	0-00, 3,7 V, 210 µs, 130 Hz	0-00, 3,7 V, 210 µs,130 Hz
3	51	m	16	Cervical	4	1	−000, 4,0 V, 150 µs, 130 Hz	0-00, 4,5 V, 150 µs, 130 Hz
4	73	f	15	Multifocal	85	13	−000,3,0 V, 180 µs, 130 Hz	−000, 3,0 V, 180 µs, 130 Hz
5	75	m	8	Multifocal	30	15	−+00, 4,5 V, 180 µs, 130	−+00, 3,0 V, 180 µs, 130
6	56	f	8	Cervical	4	1	−000, 3,0 V, 180 µs, 130 Hz	−000, 3,0 V, 180 µs, 130 Hz
7	73	f	8	Meige	17	2	0-00, 120 µs, 130 Hz, 2,0 V	0-00, 120 µs, 130 Hz, 2,0
8	62	f	5	Meige	25	3	−000, 1,8 V, 90 µs, 130 Hz	−000, 1,8 V, 90 µs, 130 Hz
9	67	f	8	Blepharospasm	8	1	−000, 2,5 V, 90 µs, 130 Hz	−000, 2,5 V, 90 µs, 130 Hz
10	36	m	33	Multisegmental	92	25	−000, 3,2 V, 90 µs, 130 Hz	−000, 2,9 V, 90 µs, 130 Hz

[a]BFMDRS: Burke–Fahn–Marsden-Dystonia-Rasting Scale.

Burke–Fahn–Marsden–Dystonia-Rating-Scale, by an experienced movement disorder specialist (K.B.) preoperatively and postoperatively and at follow-up visits.

Data Acquisition

Preoperatively, patients received MRI scans on a 3.0T Signa Exite HD GE scanner using a 8-channel head-coil. Scans included T1-weighted volumetric sequences (TE 3,2, TR 6,6, slices 180, slice thickness 1,0, matrix 240 × 240) and diffusion MRI sequences (20 directions, 2 mm, 66 axial slices, SENSE factor 2, *b*-value 1000 s/mm^{-2}). Postoperatively, patients received high-resolution CT-scans for electrode localisation.

Data Processing

Data processing was performed using FSL 5.1.2 [Jenkinson et al., 2012]. Diffusion data pre-processing involved the following steps: (1) eddy-current and head motion correction, (2) brain extraction, (3) fitting diffusion tensors on corrected 4D-data, (4) fitting a probabilistic Bayesian diffusion model on corrected data [Behrens et al., 2003, 2007]. Co-registrations of anatomic and diffusion data and normalisation to standard space were performed applying linear and nonlinear transformations [Jenkinson and Smith, 2001; Jenkinson et al., 2012]. A detailed list of coregistration parameters is presented as Supporting Information.

In parallel, diffusion MRI processing was done as in [Girard et al., 2014], based on the Diffusion in Python (Dipy—www.dipy.org) [Garyfallidis et al., 2014]. After eddy correction as done in Step 1 above, diffusion images were denoised with nonlocal means filter adapted to Rician noise [Descoteaux et al., 2008]. Then, fiber orientation distribution functions (fODFs) of order 6 were reconstructed with constrained spherical deconvolution [Descoteaux et al., 2009; Tournier et al., 2007]. The T1 anatomy was registered with SyN registration algorithm available in ANTS [Avants et al., 2009]. Then, the white/gray matter interface was extracted using FSL *fast* command and probabilistic particle filtering tractography with anatomical priors was ran with three seeds per voxel of the white matter/grey matter interface leading to full brain tractograms with approximately 1M streamlines. Default parameters were used as optimized in [Girard et al., 2014].

Electrode Segmentation

DBS electrodes were segmented as described in detail by Moreira et al. [2015]. Then, electrodes were coregistered to diffusion space. For each hemisphere, the activated electrode contact, which was shown to promote best clinical effect, was selected. This electrode contact will be referred to as "activated electrode." As a reference, we selected the most distant electrode contact, which will be referred to as "reference electrode."

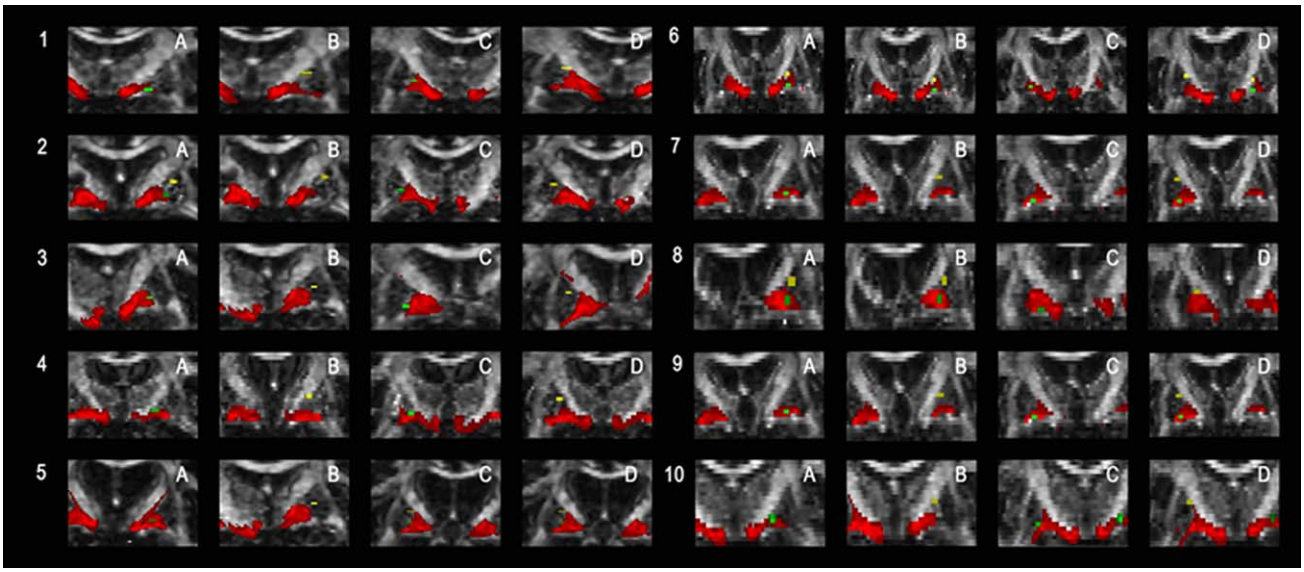

Figure 1.

Shows the topographic relationship of the pallidothalamic tracts, as obtained by probabilistic tracking, and the DBS electrodes for each patient. Activated DBS electrodes are marked in green, reference electrodes in yellow and the pallidothalamic tracts in red. [Color figure can be viewed at wileyonlinelibrary.com]

Mask Selection

Masks of the pallidum and the thalamus, available within the FSL atlas tools, were selected on the MNI template. The *lamina interna*, which is visually discernible on the MNI template, served to distinguish the internal and external pallidal segments [Beukema et al., 2015]. The masks were coregistered to each patient's diffusion scan, applying linear and nonlinear transformations between the template and individual diffusion space [Jenkinson and Smith, 2001; Jenkinson et al., 2012].

Fibre Tracking

Probabilistic *bedpostx* tractography was initiated from each patient's GPi mask for each hemisphere within individual diffusion space. To especially delineate the pallidothalamic tracts, the thalamic mask was set as a waypoint mask. For streamline-based particle filtering tracking (PFT), these regions were used as ROI filters to select streamlines from the whole tractogram going through them. Details of tractography parameters are presented as Supporting Information. Hence, two advanced probabilistic tractography algorithms publicly available will be compared; (i) FSL's bedpostx, which is extensively used in the literature and, (ii) PFT with anatomical priors, which is a streamline-based technique starting to make its way into connectivity and connectomics in the literature [Ghaziri et al., 2015; Smith et al., 2015]. To the best of our knowledge, such a comparison of algorithms and the use of streamline-based PFT algorithm is applied for the first time on DBS patients [Ghaziri et al., 2015]. This streamline-based particle filtering tractography (PFT) seeded from the white matter/grey matter interface was shown to reduce tractography length and size biases and limitations [Girard et al., 2014] in making sure that streamline connect cortical or subcortical areas, or exit the brainstem, and do not stop in anatomically invalid areas such as white matter or cortico-spinal fluid (ventricles).

RESULTS

Clinical Outcome

Patient characteristics and clinical outcome after operation are summarised in Table I. All patients had benefited from DBS. Stimulation parameters are presented in Table I.

Delineation of the Pallidothalamic Tracts

For each patient and hemisphere, we were able to delineate the pallidothalamic tracts as the fibres coursing from the GPi to the thalamus (Figs. 1 and 2). In accordance with previous descriptions, we saw them emerge the GPi at its ventral and medial border, cross the internal capsule in a diagonal angle and turn a sharp loop before entering the ventral-anterior thalamus.

Tractography results yielded consistent results across both tractography methods concerning the fibre origin from the ventral GPi and their course across the internal capsule. Streamline tractography is based on many seeds being

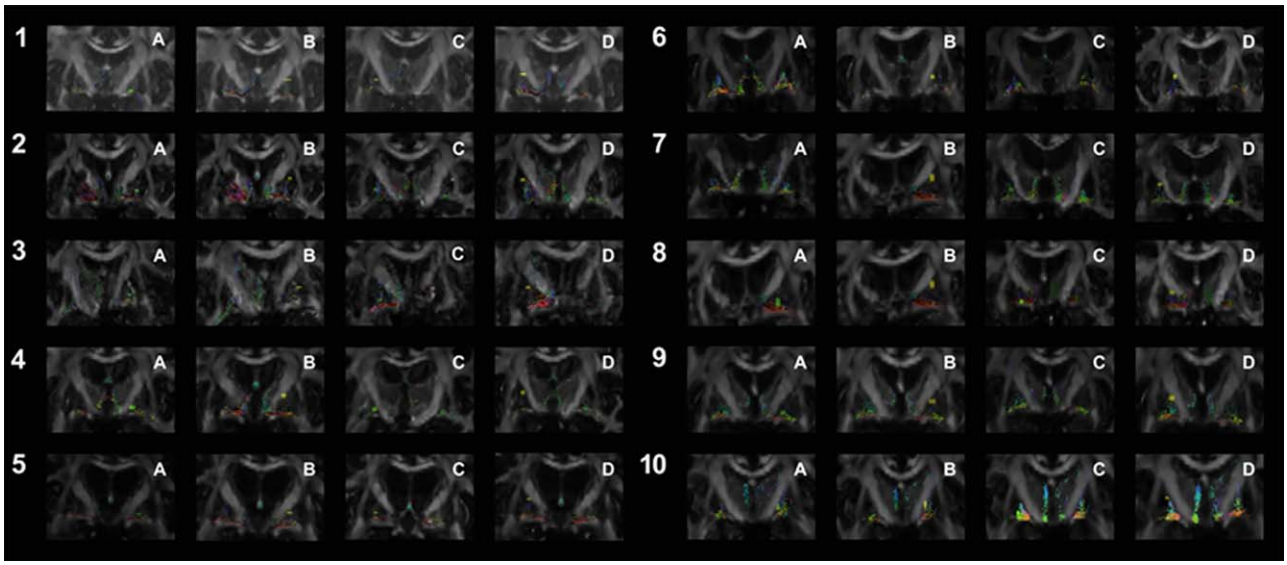

Figure 2.
Shows the topographic relationship of the pallidothalamic tracts, as obtained by streamline tracking, and the DBS electrodes for each patient. Numbering and colour codes are as in Figure 1. [Color figure can be viewed at wileyonlinelibrary.com]

launched along a tract, with the principal tract direction resulting from the fODF distribution. A streamline is generated for each seed that has been launched.

Unlike probabilistic tracking, streamline tracking enabled a distinction between the two subcomponents of the tracts, the *ansa lenticularis* and the *fasciculus lenticularis* (Fig. 2). This distinction was enhanced by providing the principal direction of the fODF view of the fibre tracts for patient Nr 2 (Fig. 3; Figure A–C arranged in anterior–posterior distribution). The ansa lenticularis as the ventral division of the pallidothalamic tract emerged from the GPi at its ventral and lateral border, to take a medially oriented descending course before crossing the internal capsule in a sharp loop. The dorsal division of the fibre bundle, the lenticular fasciculus, left the GPi more medially and dorsally to the *ansa lenticularis* and crossed the internal capsule directly and without a sharp loop.

Topography of Electrodes and Fibres

In order to characterise the topographic relationship between DBS electrodes and the course of the pallidothalamic fibres, the activated and reference DBS electrodes were superimposed on the pallidothalamic tracts in each patient's diffusion space (Figs. 1 and 2). The distance between the electrodes and the pallidothalamic tracts was calculated

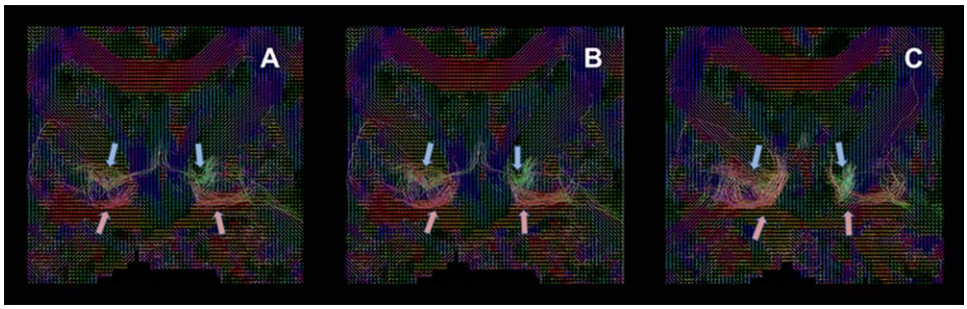

Figure 3.
Presents the fiber orientation distribution functions (fODFs), indicating the principal streamline direction for each voxel, in patient 2. Directionality of the principal tractography vector is coded in colour (green: anterior–posterior; red: interhemispheric; blue: descending). The ansa lenticularis is marked by a red arrow, the faciculus lenticularis by a blue one. **A–C** are arranged from anterior to posterior. [Color figure can be viewed at wileyonlinelibrary.com]

TABLE II. Presents the distance in mm between electrodes and the pallidothalamic tracts, as obtained by streamline tracking

Patient Nr	Left ventral	Left dorsal	Right ventral	Right dorsal
1	7	13	0	10
2	0	13	7	8
3	0	8	6	13
4	0	12	4	11
5	0	0	4	9
6	0	7	0	12
7	0	11	6	13
8	0	10	0	6
9	0	8	0	10
10	0	9	0	9
Mean	1	9	3	10

(Tables II and III). For distance calculation, we did not take fibres of passage within the internal capsule into account, but only the pallidothalamic tracts at the ventral GPi border. Different results across both methods are due to the fact that a clear delineation of the pallidothalamic tracts and fibres of passage is not possible with the probabilistic fibre tracking approach.

For the activated DBS electrodes, we found a very close association to the pallidothalamic tracts: these electrodes were situated at a distance of 0–3 mm away from the tracts, whereas the reference electrodes were localised 9–12 mm away. Group differences turned out to be statistically significant applying SPSS 23.0 (streamline tracking: left side: $P = 0.00073$; right side: $P = 0{,}00028$; probabilistic tracking: left side: $P = 00009$; right side: $P = 0{,}00008$).

These findings indicate a strong anatomical vicinity of activated DBS electrodes and the pallidothalamic tracts, in particular the ansa lenticularis.

TABLE III. Presents the distance in mm between electrodes and the pallidothalamic tracts, as obtained by probabilistic tracking

Patient Nr	Left ventral	Left dorsal	Right ventral	Right dorsal
1	0	14	0	17
2	0	14	6	11
3	0	11	0	11
4	0	9	0	12
5	0	3	0	10
6	0	6	0	13
7	0	12	0	10
8	0	7	0	11
9	0	8	0	12
10	0	8	0	10
Mean	0	9	1	12

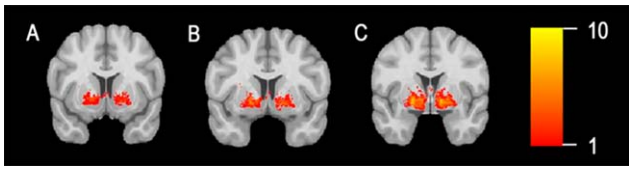

Figure 4.
Illustrates the interindividual variability of tract course across subjects. A sum of binarised tracts, as obtained by streamline tracking, is provided for the anterior (A), middle (B), and posterior (C) GPi. The degree of overlap across patients is coded in colour. [Color figure can be viewed at wileyonlinelibrary.com]

Interindividual Variability

Interindividual variability of the anatomic course of fibre tracts was illustrated by presenting a binarised overlap image for the tracts obtained by streamline tracking across the group (Fig. 4). Overlap was highest along the ventral borders of the posterior GPi, then passing through the internal capsule. For the anterior and middle GPi, we saw a reduced degree of overlap.

DISCUSSION

Main Findings

In this study, we examined the topographic relationship of clinically efficient DBS electrodes and the pallidothalamic tracts in ten dystonia patients. We discovered a close vicinity of clinically efficient DBS electrodes and the pallidothalamic tracts, in particular the *ansa lenticularis*. Applying advanced streamline tractography, we were able to in vivo delineate the subdivisions of the pallidothalamic tracts for the first time.

Anatomy of the Pallidothalamic Tracts

Much of our knowledge on the course of the pallidothalamic tracts depends on tracer labelling studies in primates. There have been controversial debates as to the origin and course of the fibres: one group claims the *fasciculus lenticularis* to emerge from posterior and posterolateral portions of the GPi [Baron et al., 2001, 2006; Kim et al., 1976; Ranson and Ranson, 1939], whereas the *ansa lenticularis* stems from anterior and was seen to exit the GPi at its medial border [Baron et al., 2001]. Another group, however, postulates the *ansa lenticularis* to emerge from the lateral GPi and the *fasciculus lenticularis* to emerge from the medial GPi [Parent and Hazrati, 1995; Parent and Parent, 2004]. According to that concept, the *fasciculus lenticularis* courses dorsomedially to the *ansa lenticularis*, and both tracts merge into the *fascisulus thalamicus* within Forel's field H1.

Human data is scarce and, at present, limited to one detailed postmortem analysis of three human brains [Gallay et al., 2008]. There, the pallidothalamic tracts were be

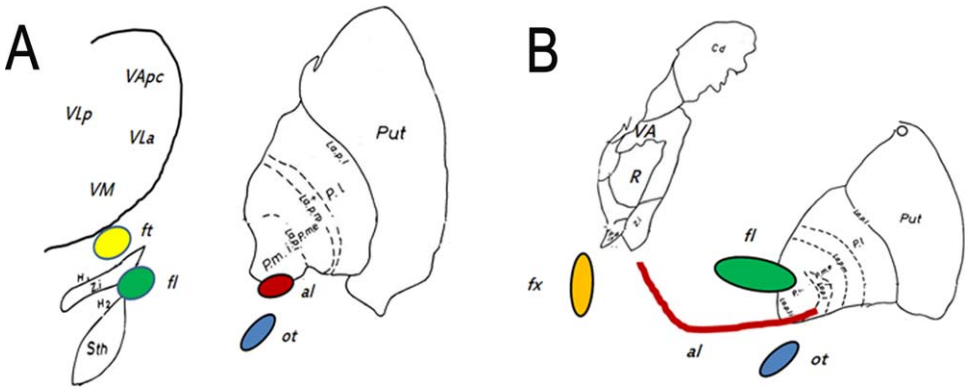

Figure 5.
Illustrates the topography of the pallidothalamic tracts presented on the Schaltenbrand–Wahren atlas. (**A**) presents a view 1.5 mm anterior to the midcommissural point, (**B**) 5.5 mm anterior. [Color figure can be viewed at wileyonlinelibrary.com]

composed of a ventral part, the *ansa lenticularis*, which originates from the anteroventral border of the GPi just above the optic tract, then to cross the internal capsule and form a sharp upward loop. The dorsal part, on the other hand, was seen to run dorsal to the subthalamic nucleus within Forel's field H1. Before entering the thalamus, both fibre bundles merge into the *fasciculus thalamicus*. Concerning interindividual variability, overlap appeared highest in the dorsoventral and anterior–posterior directions, but not in mediolateral extension. Figure 5 presents a schematic drawing of the pallidothalamic tracts and their topographic relation to the fornix and optic tract, adapted to the Schaltenbrand–Wahren [Niemann et al., 1994] atlas and imaging results of the human brain [Gallay et al., 2008].

Our results are similar to the scheme of the pallidothalamic tracts proposed by Parent et al. [Parent and Parent, 2004], with the *ansa lenticularis* emerging from the anterior and lateral GPi, as opposed to a more dorsal and medial origin for the *fasciculus lenticularis*. Due to the limitations of diffusion MRI within grey matter, we cannot provide statements on axonal courses within the GPi.

Role of the Pallidothalamic Tracts in DBS

Pathophysiologically, the pallidothalamic tracts constitute the main GPi efferent pathways and thus basal ganglia output to the thalamus. Functionally, the GPi acts as an important relay station within the direct basal ganglia pathway that disinhibits the thalamus and thereby facilitates movement [Alexander and Crutcher, 1990]. It is one of the paradoxes of functional neurosurgery why lesioning of the GPi and its efferent pathways alleviates hyperkinetic movements [Brown and Eusebio, 2008] and why integrity of the pallidothalamic tracts should be a required precondition for hemiballism to emerge [Whittier and Mettler, 1949]. Arguments towards a synchronisation of oscillation patterns have been brought forward here [Hutchison et al., 2004]. Also, induction of hypokinetic conditions and postural instability was seen during GPi DBS that successfully alleviated dystonic symptoms [Brecl Jakob et al., 2015].

Methodological Differences

There are important methodological differences between probabilistic *bedpostx*-like tractography and streamline-based methods, but both essentially try to account for the uncertainty in the principal directions estimated from the diffusion data. In streamline-based methods, the probabilistic aspect of the algorithm is the choice of the local direction to be followed at every voxel. Streamline tracking launches many seeds and lets them move along the tract by randomly picking a direction at each step following the fODF distribution and uncertainty in the principal directions. The result is a streamline for every seed launched. Due to the higher resolution of seeds, we were able to distinguish both sub-divisions of the tracts, which differ in their principal direction. Probabilistic bedpostx tractography is similar, but the biggest difference is that, from a seed point, bedpostx creates a connectivity map (heatmap) of most probable connections to this seed by launching thousands of particles. A Bayesian model estimates uncertainty in the local directions to follow. The output is a probabilistic connectivity map that needs to be thresholded at the level of confidence desired, which, as streamline-based methods, also reflects the uncertainty in the diffusion data, and not the "*connection strength*." Therefore, we have a slight preference for the streamline-based approach in the current application as we can analyse results without having to apply thresholds on the probabilistic tracts.

Limitations of This Study and Future Perspectives

We are aware of a number of limitations that this study faces. First, as we present only structural and anatomic data, we cannot deduce results on the functional role the pallidothalamic tracts play within the basal ganglia circuit and in promoting clinical DBS effects. To address this question, functional imaging data and local field potentials would be needed to complement our findings. Second, we only included 10 patients with a high degree of variation concerning symptom distribution, age, and gender. This is primarily due to the relatively low inclusion rate of DBS dystonia patients in imaging studies as MRI images with motion artefacts do not qualify for analysis. Apart from the 10 dystonia patients included in this study, five additional dystonia patients had undergone DBS surgery in our hospital. Owing to motion artefacts, their images could not be included in this study. During the operation, the stereotactic frame impedes the acquisition of diffusion images, and a second general anaesthetic procedure solely for image acquisition is ethically not tenable. Also, a postoperative acquisition of diffusion scans is impaired by the implanted stimulation device. Therefore, we intend to conduct a multicentre study including a higher number of clinically more homogeneous patients.

CONCLUSIONS

In this study, we were able to show a close **anatomic vicinity** of clinically efficient DBS electrodes and the pallidothalamic tracts in dystonia patients. Therefore, we propose the pallidothalamic tracts to be the major fibre bundle targeted by DBS in dystonia. Intraoperative electrophysiological recordings would be needed to complement our anatomic findings with functional evidence. In the future, a clear and individual delineation of the pallidothalamic tracts could optimize the stereotactic process of optimal electrode localization.

REFERENCES

Alexander GE, Crutcher MD (1990): Functional architecture of basal ganglia circuits: Neural substrates of parallel processing. Trends Neurosci 13:266–271.

Avants BB, Tustison NJ, Song G, Gee JC (2009): ANTS: Advanced Open-Source Normalization Tools for Neuroanatomy. Philadelphia: Penn Image Computing and Science Laboratory.

Baron MS, Sidibe M, DeLong MR, Smith Y (2001): Course of motor and associative pallidothalamic projections in monkeys. J Comp Neurol 429:490–501.

Baron MS, Noonan JB, Mewes K (2006): Restricted ablative lesions in motor portions of GPi in primates produce extensive loss of motor-related neurons and degeneration of the lenticular fasciculus. Exp Neurol 202:67–75.

Behrens TE, Johansen-Berg H, Woolrich MW, Smith SM, Wheeler-Kingshott CA, Boulby PA, Barker GJ, Sillery EL, Sheehan K, Ciccarelli O, Thompson AJ, Brady JM, Matthews PM (2003): Non-invasive mapping of connections between human thalamus and cortex using diffusion imaging. Nat Neurosci 6: 750–757.

Behrens TE, Berg HJ, Jbabdi S, Rushworth MF, Woolrich MW (2007): Probabilistic diffusion tractography with multiple fibre orientations: What can we gain? Neuroimage 34:144–155.

Beukema P, Yeh FC, Verstynen T (2015): In vivo characterization of the connectivity and subcomponents of the human globus pallidus. Neuroimage 120:382–393.

Brecl Jakob G, Pelykh O, Košutzká Z, Pirtošek Z, Trošt M, Ilmberger J, Valkovic P, Mehrkens JH, Bötzel K (2015): Postural stability under globus pallidus internus stimulation for dystonia. Clin Neurophysiol 126:2299–2305.

Brown P, Eusebio A (2008): Paradoxes of functional neurosurgery: Clues from basal ganglia recordings. Mov Disord 23:12–20. quiz 158.

Coenen VA, Allert N, Madler B (2011): A role of diffusion tensor imaging fiber tracking in deep brain stimulation surgery: DBS of the dentato-rubro-thalamic tract (drt) for the treatment of therapy-refractory tremor. Acta Neurochir 153:1579–1585; discussion 85. (Wien)

Coenen VA, Panksepp J, Hurwitz TA, Urbach H, Madler B (2012): Human medial forebrain bundle (MFB) and anterior thalamic radiation (ATR): Imaging of two major subcortical pathways and the dynamic balance of opposite affects in understanding depression. J Neuropsychiatry Clin Neurosci 24:223–236.

Descoteaux M, Wiest-Daessle N, Prima S, Barillot C, Deriche R (2008): Impact of Rician adapted Non-Local Means filtering on HARDI. Med Image Comput Comput Assist Interv 11(Pt 2):122–130.

Descoteaux M, Deriche R, Knosche TR, Anwander A (2009): Deterministic and probabilistic tractography based on complex fibre orientation distributions. IEEE Trans Med Imaging 28: 269–286.

Gallay MN, Jeanmonod D, Liu J, Morel A (2008): Human pallidothalamic and cerebellothalamic tracts: Anatomical basis for functional stereotactic neurosurgery. Brain Struct Funct 212: 443–463.

Garyfallidis E, Brett M, Amirbekian B, Rokem A, van der Walt S, Descoteaux M, Nimmo-Smith I; Dipy Contributors (2014): Dipy, a library for the analysis of diffusion MRI data. Front Neuroinform 8:8.

Ghaziri J, Tucholka A, Girard G, Houde JC, Boucher O, Gilbert G, Descoteaux M, Lippé S, Rainville P, Nguyen DK (2015): The corticocortical structural connectivity of the human insula. Cereb Cortex 25:162:1256–1265.

Girard G, Whittingstall K, Deriche R, Descoteaux M (2014): Towards quantitative connectivity analysis: Reducing tractography biases. Neuroimage 98:266–278.

Hunsche S, Sauner D, Runge MJ, Lenartz D, El Majdoub F, Treuer H, Sturm V, Maarouf M (2013): Tractography-guided stimulation of somatosensory fibers for thalamic pain relief. Stereotact Funct Neurosurg 91:328–334.

Huss DS, Dallapiazza RF, Shah BB, Harrison MB, Diamond J, Elias WJ (2015): Functional assessment and quality of life in essential tremor with bilateral or unilateral DBS and focused ultrasound thalamotomy. Mov Disord 30:1937–1943.

Hutchison WD, Dostrovsky JO, Walters JR, Courtemanche R, Boraud T, Goldberg J, Brown P (2004): Neuronal oscillations in the basal ganglia and movement disorders: Evidence from whole animal and human recordings. J Neurosci 24:9240–9243.

Jenkinson M, Smith S (2001): A global optimisation method for robust affine registration of brain images. Med Image Anal 5: 143–156.

Jenkinson M, Beckmann CF, Behrens TE, Woolrich MW, Smith SM (2012): FSL. Neuroimage 62:782–790.

Kim R, Nakano K, Jayaraman A, Carpenter MB (1976): Projections of the globus pallidus and adjacent structures: An autoradiographic study in the monkey. J Comp Neurol 169:263–290.

Klein JC, Barbe MT, Seifried C, Baudrexel S, Runge M, Maarouf M, Gasser T, Hattingen E, Liebig T, Deichmann R, Timmermann L, Weise L, Hilker R (2012): The tremor network targeted by successful VIM deep brain stimulation in humans. Neurology 78:787–795.

Kocabicak E, Temel Y, Hollig A, Falkenburger B, Tan S (2015): Current perspectives on deep brain stimulation for severe neurological and psychiatric disorders. Neuropsychiatr Dis Treat 11:1051–1066.

Krack P, Pollak P, Limousin P, Hoffmann D, Benazzouz A, Le Bas JF, Koudsie A, Benabid AL (1998): Opposite motor effects of pallidal stimulation in Parkinson's disease. Ann Neurol 43: 180–192.

Kupsch A, Benecke R, Müller J, Trottenberg T, Schneider GH, Poewe W, Eisner W, Wolters A, Müller JU, Deuschl G, Pinsker MO, Skogseid IM, Roeste GK, Vollmer-Haase J, Brentrup A, Krause M, Tronnier V, Schnitzler A, Voges J, Nikkhah G, Vesper J, Naumann M, Volkmann J; Deep-Brain Stimulation for Dystonia Study Group (2006): Pallidal deep-brain stimulation in primary generalized or segmental dystonia. N Engl J Med 355:1978–1990.

Kupsch A, Tagliati M, Vidailhet M, Aziz T, Krack P, Moro E, Krauss JK (2011): Early postoperative management of DBS in dystonia: Programming, response to stimulation, adverse events, medication changes, evaluations, and troubleshooting. Mov Disord 26 Suppl 1:S37–S53.

Lauro PM, Vanegas-Arroyave N, Huang L, Taylor PA, Zaghloul KA, Lungu C, Saad ZS, Horovitz SG (2016): DBSproc: An open source process for DBS electrode localization and tractographic analysis. Hum Brain Mapp 37:422–433.

Machado A, Rezai AR, Kopell BH, Gross RE, Sharan AD, Benabid AL (2006): Deep brain stimulation for Parkinson's disease: Surgical technique and perioperative management. Mov Disord 21 Suppl 14:S247–S258.

Mehrkens JH, Bötzel K, Steude U, Zeitler K, Schnitzler A, Sturm V, Voges J (2009): Long-term efficacy and safety of chronic globus pallidus internus stimulation in different types of primary dystonia. Stereotact Funct Neurosurg 87:8–17.

Moreira da Silva N, Rozanski VE, Silva Cunha JP (2015): A 3D multimodal approach to precisely locate DBS electrodes in the basal ganglia brain region. IEEE Conf Proc 2015:292–295.

Niemann K, Naujokat C, Pohl G, Wollner C, von Keyserlingk D (1994): Verification of the Schaltenbrand and Wahren stereotactic atlas. Acta Neurochir (Wien) 129:72–81.

Parent A, Hazrati LN (1995): Functional anatomy of the basal ganglia. I. The cortico-basal ganglia-thalamo-cortical loop. Brain Res Brain Res Rev 20:91–127.

Parent M, Parent A (2004): The pallidofugal motor fiber system in primates. Parkinsonism Relat Disord 10:203–211.

Ranson SW, Ranson M (1939): Pallidofugal fibers in the monkey. AMA ArchNeurol Psychiatry 42:1059–1067.

Rozanski VE, Vollmar C, Cunha JP, Tafula SM, Ahmadi SA, Patzig M, Mehrkens JH, Bötzel K (2014): Connectivity patterns of pallidal DBS electrodes in focal dystonia: A diffusion tensor tractography study. Neuroimage 84:435–442.

Smith RE, Tournier JD, Calamante F, Connelly A (2012): Anatomically-constrained tractography: Improved diffusion MRI streamlines tractography through effective use of anatomical information. Neuroimage 62:1924–1938.

Smith RE, Tournier JD, Calamante F, Connelly A (2015): The effects of SIFT on the reproducibility and biological accuracy of the structural connectome. Neuroimage 104:253–265.

Tournier JD, Calamante F, Connelly A (2007): Robust determination of the fibre orientation distribution in diffusion MRI: Non-negativity constrained super-resolved spherical deconvolution. Neuroimage 35:1459–1472.

Vanegas-Arroyave N, Lauro PM, Huang L, Hallett M, Horovitz SG, Zaghloul KA, Lungu C (2016): Tractography patterns of subthalamic nucleus deep brain stimulation. Brain 139(Pt 4): 1200–1210.

Volkmann J, Mueller J, Deuschl G, Kühn AA, Krauss JK, Poewe W, Timmermann L, Falk D, Kupsch A, Kivi A, Schneider GH, Schnitzler A, Südmeyer M, Voges J, Wolters A, Wittstock M, Müller JU, Hering S, Eisner W, Vesper J, Prokop T, Pinsker M, Schrader C, Kloss M, Kiening K, Boetzel K, Mehrkens J, Skogseid IM, Ramm-Pettersen J, Kemmler G, Bhatia KP, Vitek JL, Benecke R; DBS study group for dystonia (2014): Pallidal neurostimulation in patients with medication-refractory cervical dystonia: A randomised, sham-controlled trial. Lancet Neurol 13:875–884.

Whittier JR, Mettler FA (1949): Studies on the subthalamus of the rhesus monkey; hyperkinesia and other physiologic effects of subthalamic lesions; with special reference to the subthalamic nucleus of Luys. J Comp Neurol 90:319–372.